

Evidence for Fe^{4+} in $\text{YBa}_2(\text{Cu}_{1-x}\text{M}_x)_3\text{O}_{7-y}$ ($M = {}^{57}\text{Fe}, {}^{57}\text{Co}$) by absorption and emission Mössbauer spectroscopy

L. Bottyán, B. Molnár, D. L. Nagy, I. S. Szücs, and J. Tóth
Central Research Institute for Physics, H-1525 Budapest, P.O. Box 49, Hungary

J. Dengler, G. Ritter, and J. Schober

*Physikalisches Institut der Universität Erlangen-Nürnberg, Glückstrasse 10, D-8520 Erlangen,
Federal Republic of Germany*

(Received 15 July 1988)

${}^{57}\text{Fe}$ absorption and ${}^{57}\text{Co}$ emission Mössbauer spectroscopy were applied to iron- and cobalt-doped $\text{YBa}_2(\text{Cu}_{1-x}\text{M}_x)_3\text{O}_{7-y}$ high-temperature superconductors ($M = {}^{57}\text{Fe}, {}^{57}\text{Co}$; $3.5 \times 10^{-5} \leq x \leq 0.1$, $y=0$ and $y=0.8$) between 4.2 and 295 K with and without external magnetic field. Four iron species *A*, *B*, *C*, and *D*, are observed with different dominance at different x and y . Aftereffects of the electron capture are ruled out. At 4.2 K, spontaneous antiferromagnetic order is shown by contributions *A*, *B*, and *C* in spectra of samples with $x_{\text{Fe}} \geq 0.06$. A model-independent separation of the magnetically split subspectra shows an asymmetry parameter of the electric field gradient above 0.8 for *A* and *B*. Temperature and external magnetic field dependence of the magnetic splittings is indicative of superparamagnetic relaxation of small clusters. The species *A*, *B*, and *C* are magnetically interrelated. We suggest a preferential Cu(1) substitution by Fe and Co. Three of the four iron species, viz. *A*, *B*, and *D*, have been assigned to high-spin Fe^{4+} ; *C* is high spin Fe^{3+} . We provide evidence that Co is mostly in the four-valent state, too. Four-valent Fe and Co substitution in $\text{YBa}_2\text{Cu}_3\text{O}_{7-y}$ is in reasonable agreement with the dopant concentration dependence of T_c . Possible crystallographic assignments of all four iron (cobalt) sites are discussed.

INTRODUCTION

In spite of the great deal of endeavor of many groups worldwide, the origin of Cooper pairing in the high- T_c oxide superconductors still remains to be elucidated. $\text{YBa}_2\text{Cu}_3\text{O}_{7-y}$ (often referred to as the 1:2:3 compound) has a threefold stacked orthorhombic perovskite structure where the central unit contains Y while the others contain Ba.¹⁻³ There exist two different Cu sites, Cu(1) located between two Ba-O(4) planes, and Cu(2) between the Y and Ba-O(4) planes. The coordination of Cu(1) depends on the oxygen stoichiometry. For $y=0$ in the pure 1:2:3 compound, which is a 90-K superconductor, Cu(1)-O(1) chains are formed leaving the $(0, \frac{1}{2}, 0)$ sites [O(5)] practically unoccupied,³ so Cu(1) has a fourfold coordinated square-planar environment. On reducing the sample, oxygen is removed from the basal [O(1)-Cu(1)-O(5)] plane³ (i.e., from the chains). Superconductivity disappears with the onset of tetragonality around $y=0.5$.³

Systematic atomic substitution studies in the 1:2:3 compound have provided additional understanding of these materials. Replacement of Y by different and even strongly magnetic rare earths has a minor effect on T_c ,^{4,5} indicating that the rare-earth site is isolated from the Cu(2)-O network, the superconducting region in these substances.⁶ $3d$ elements substituting on the Cu site substantially diminish T_c .⁷ This T_c diminution is correlated with the shortening of the Cu(1)-O(4) bond length in both doped and undoped $\text{YBa}_2\text{Cu}_3\text{O}_{7-y}$, indicating that T_c depression is related to the details of the chemical bonds among the ions, and less affected by the presence of

paramagnetic substitutional ions.⁸

Samples with dopant concentrations of up to $x_{\text{Fe}}=0.27$ and $x_{\text{Co}}=0.33$ were found to be of single phase.⁷ By increasing the Fe or Co concentration the structure becomes tetragonal^{7,9} with a threshold value for both Fe and Co of about $x=0.025$.⁷⁻¹¹ However, x -induced tetragonality is qualitatively different from that induced by oxygen removal (y -induced tetragonality) in the undoped 1:2:3 compound, since superconductivity persists at low temperatures in the tetragonal phase of doped 1:2:3 systems.⁷⁻¹¹ Diffraction studies of Fe- and Co-doped tetragonal 1:2:3 compounds ($x_{\text{dopant}} \approx 0.05, 0.07, \text{ and } 0.08$) revealed that Fe and Co preferentially substitute at Cu(1) sites and that excess oxygen is brought into the lattice in an amount increasing with increasing Fe and Co concentration.^{8,12,13} The oxidized x -induced tetragonal 1:2:3 compound is considered as an assembly of heavily and incoherently twinned orthorhombic individuals being tetragonal only in a statistical sense.¹² Diffraction data on $\text{YBa}_2(\text{Cu}_{0.92}\text{Fe}_{0.08})_3\text{O}_{7-y}$ were interpreted by chainlike Fe(1) clusters along the [110] direction.¹³ It is remarkable that Fe- and Co-doping results in the same changes of crystallographic data and T_c at almost the same x values.

Substitution at Cu sites studied by resonance methods revealing local atomic arrangements is therefore of special interest. Several authors reported on ${}^{57}\text{Fe}$ Mössbauer spectroscopy results on $\text{YBa}_2(\text{Cu}_{1-x}\text{Fe}_x)_3\text{O}_{7-y}$. Spectra of samples with $x_{\text{Fe}} > 0.02$ published so far comprise at least three different doublets, viz. *A*, *B*, and *C*, at room temperature with quadrupole splittings of 1.93–2.0, 1.07–1.3, and 0.26–0.7 mm/s and isomer shifts of

0.03–0.09, –0.02–0.08, and 0.2–0.35 mm/s, respectively.^{14–22} Doublet *A* is dominant in the reduced (semiconducting) state and *B* in the oxidized (superconducting) state. Intensity fraction of doublet *C* remains low. A fourth species, i.e., *D*, was suggested by Baggio-Saitovitch *et al.*,¹⁵ by us,¹⁶ and recently by Blue *et al.*¹⁷ for low *x* and low *y* with a quadrupole splitting of 1.6 mm/s and an isomer shift of –0.19 mm/s at room temperature.

Here we report on Mössbauer emission and absorption studies of doped $\text{YBa}_2(\text{Cu}_{1-x}\text{M}_x)_3\text{O}_{7-y}$ ($\text{M} = {}^{57}\text{Co}$ and ${}^{57}\text{Fe}$). Samples with dopant concentrations $x_{\text{Co}} = 3.5 \times 10^{-5}$ and $x_{\text{Fe}} = 0.0015, 0.01, 0.06,$ and 0.1 were investigated. Representative spectra will be shown here; a more detailed Mössbauer study of these materials will be published at a later date.

EXPERIMENT

Materials were prepared by firing stoichiometric quantities of high-purity Y_2O_3 , BaCO_3 , and $\text{CuO}(\text{Fe},\text{Co})$ in two steps. CuO powder was first dropped by an aqueous solution of ${}^{57}\text{CoCl}_2$ or ${}^{57}\text{FeCl}_2$. The dried and mixed powder was heated to 950°C in air for 2 h to convert the chloride into fine-grained oxide and cooled to room temperature in 1 h. Then the product was reground, pressed into pellets, fired at 1020°C in oxygen for 2 h, cooled to room temperature in 2 h, and divided into two sets. The first set prepared as above was used for the first set of Mössbauer probes (“oxidized state,” $y \approx 0$). The second set of samples was further heat treated in Ar flow at 480°C for 17 h. Such treatment results in a loss of oxygen and a suppression of superconductivity (“reduced state,” $y \approx 0.8$).

The probes were characterized by x-ray diffraction and resistivity measurements. In the case of the ${}^{57}\text{Co}$ -doped substance a nonradioactive parallel probe was used. No residual phase was detected by x-ray diffraction (detection limit 5%). Unit-cell dimensions showed a dependence on the iron content similar to that reported by others.⁷ The samples with $x_{\text{Co}} = 3.5 \times 10^{-5}$, $x_{\text{Fe}} = 0.0015$, and $x_{\text{Fe}} = 0.01$ were found to be orthorhombic and superconducting in the oxidized state and tetragonal with an ever increasing resistivity down to 10 K in the reduced state. A tetragonal pattern was found for $x_{\text{Fe}} = 0.06$ and $x_{\text{Fe}} = 0.1$ in both oxidized (superconducting) and reduced (nonsuperconducting) states. Temperature dependence of the electric conductivity of the oxidized state samples showed superconducting transitions centered at the temperatures 89, 88, 84, 56, and 21 K, for dopant concentrations $x_{\text{Co}} = 3.5 \times 10^{-5}$, $x_{\text{Fe}} = 0.0015$, $x_{\text{Fe}} = 0.01$, $x_{\text{Fe}} = 0.06$, and $x_{\text{Fe}} = 0.1$, respectively. The width of the transition was monotonously increasing with the dopant concentration.

${}^{57}\text{Fe}$ absorption and ${}^{57}\text{Co}$ emission Mössbauer spectra of powdered samples mixed with boron nitride were taken using conventional constant acceleration spectrometers. Emission spectra were recorded using a single line absorber of $\text{K}_4\text{Fe}(\text{CN})_6 \cdot 3\text{H}_2\text{O}$. Low-temperature measurements were performed in liquid-He cryostats equipped with superconducting coils and a variable temperature probe in the case of absorption measurements. Isomer

shifts are reported relative to that of $\alpha\text{-Fe}$ at room temperature.

RESULTS AND DISCUSSION

Room-temperature spectra of Fe- and Co-doped $\text{YBa}_2\text{Cu}_3\text{O}_{7-y}$ samples are shown in Fig. 1. For easy comparison the velocity scale of ${}^{57}\text{Co}$ emission spectra has been inverted. The spectra with $x_{\text{Fe}} \geq 0.06$ comprise three quadrupole doublets *A*, *B*, and *C*. For $x_{\text{Fe}} = 0.01, 0.0015$, and $x_{\text{Co}} = 3.5 \times 10^{-5}$ a contribution of doublet *D* increasing with decreasing dopant concentration is observed. Quadrupole splittings, isomer shifts, linewidths, and relative intensities of the least-squares-fitted quadrupole doublets of Lorentzians are summarized in Table I. Contribution *A* dominates Mössbauer spectra at high *y*, i.e., in the reduced state, contributions *B* and/or *D* dominate at low *y*, i.e., in the oxidized state. Intensity fraction of *C* does not vary significantly with either *x* or *y*. We point out that hyperfine parameters of *A*, *B*, and *C* show no significant variation with *y* and only little with *x* (Table I). Doublets *B* (except for $x_{\text{Fe}} = 0.06$ and $y = 0.8$) and *D* are symmetrical, *A* and *C* are slightly asymmetrical for $x_{\text{Fe}} \geq 0.06$. As, however, the total asymmetry accounts only for less than 3% of the total intensity in samples with $x_{\text{Fe}} \geq 0.06$, we shall not discuss the line asymmetries hereafter. A remarkable asymmetry of the doublets *A* and *B* ($I_1/I_2 = 1.7$ and 1.3) was observed in $\text{YBa}_2(\text{Cu}_{0.99}\text{Fe}_{0.01})_3\text{O}_{6.86}$ by Takano and Takeda¹⁴ and was attributed to the Goldanskii-Karyagin effect. Such high asymmetries, however, could only be explained by an unrealistically high degree of anisotropy of the lattice vibrations [i.e., $(\langle x^2 \rangle - \langle z^2 \rangle)^{1/2} = 0.27$ and 0.19 \AA , respectively].²³ A preferred orientation of the crystallites was ruled out by the authors themselves. The introduction of a further quadrupole doublet with isomer shift –0.16 mm/s and quadrupole splitting 1.55 mm/s at room temperature remains the only alternative explanation for the measured asymmetry. These parameters are close to those of *D* found by us at low *x*, low *y*.

In Fig. 2, ${}^{57}\text{Co}$ emission spectra revealing no spontaneous magnetic splitting at 4.2 K are shown. Spectra were computer fitted by three symmetrical quadrupole doublets *A*, *C*, and *D* (Table I). No contribution from doublet *D* was detected in the reduced state. By applying an external magnetic field of 5 T, poorly resolved magnetically split spectra are observed. The linear combination method as described below was applied to extract the magnetically split net contributions from *A* and *D*. The spectrum of the reduced sample was taken as pattern *A*, because the low intensity flat contribution of *C* is smeared out. The contributions *A* and *D* are displayed in Figs. 2(c) and 2(e). The net magnetic fields (H_{eff}) at the ${}^{57}\text{Fe}$ nucleus are about 19 and 16 T for subspectra *A* and *D*, respectively. Provided that H_{eff} is parallel or antiparallel to H_{ext} , the external magnetic field, spectra are consistent with a positive *z*-component V_{zz} of the electric-field gradient (EFG). Magnetic field spectra reveal that both *A* and *D* are paramagnetic species at 4.2 K.

Spectra of samples with $x_{\text{Fe}} = 0.1$ and 0.06 for $y = 0$ and

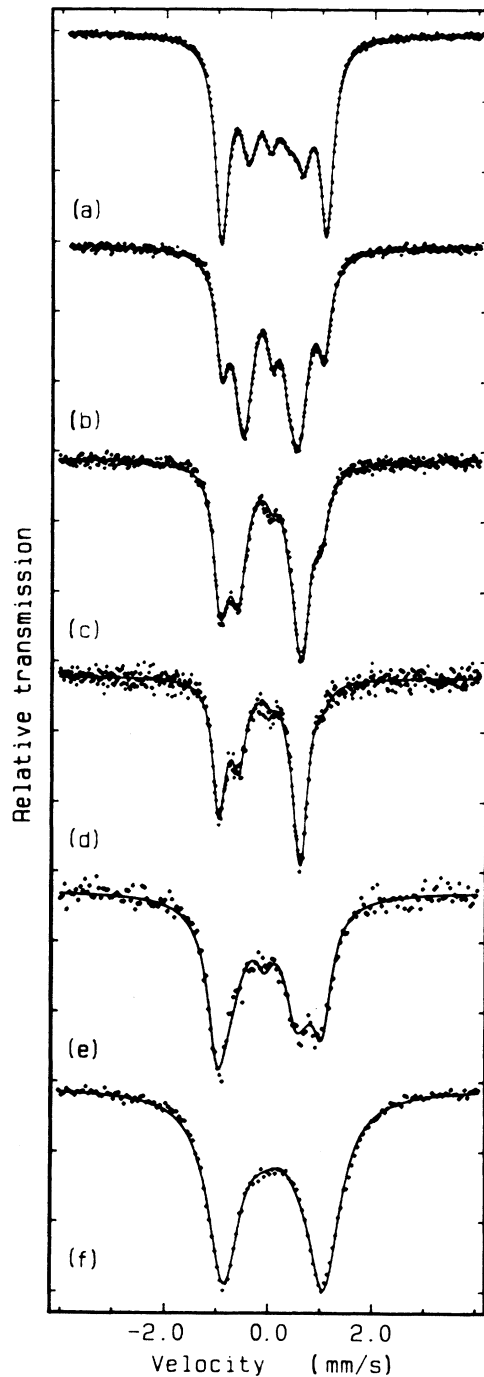


FIG. 1. Room-temperature Mössbauer absorption and emission spectra of $\text{YBa}_2(\text{Cu}_{1-x}\text{M}_x)_3\text{O}_{7-y}$ ($M = {}^{57}\text{Fe}, {}^{57}\text{Co}$). (a) $x_{\text{Fe}}=0.1, y \approx 0.8$. (b) $x_{\text{Fe}}=0.1, y \approx 0$. (c) $x_{\text{Fe}}=0.1, y \approx 0$. (d) $x_{\text{Fe}}=0.0015, y \approx 0$. (e) $x_{\text{Co}}=3.5 \times 10^{-5}, y \approx 0$. (f) $x_{\text{Co}}=3.5 \times 10^{-5}, y \approx 0.8$. Velocity scale of emission spectra inverted.

0.8 recorded at 4.2 K show spontaneous magnetic splitting. Spectra of the $x_{\text{Fe}}=0.1$ sample are displayed in Fig. 3. The magnetically split subspectrum C can easily be identified by its isomer shift of ≈ 0.4 mm/s [solid lines in Figs. 3(a) and 3(b)]. The value of H_{eff} and the sign of V_{zz} (i.e., the sign of $eQV_{zz}/2$ where Q is the quadrupole mo-

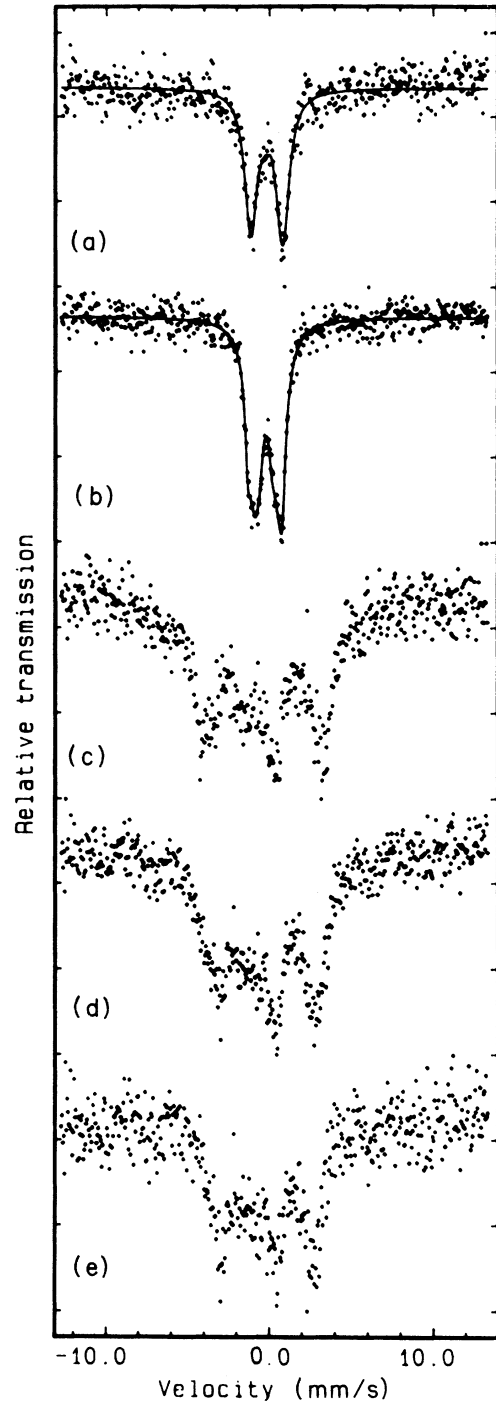


FIG. 2. Mössbauer emission spectra of $\text{YBa}_2(\text{Cu}_{1-x}{}^{57}\text{Co}_x)_3\text{O}_{7-y}$ with $x_{\text{Co}}=3.5 \times 10^{-5}$ at $T=4.2$ K without and with applied magnetic field of 5 T. (a) $y \approx 0.8, H_{\text{ext}}=0$. (b) $y \approx 0, H_{\text{ext}}=0$. (c) $y \approx 0.8, H_{\text{ext}}=5$ T. (d) $y \approx 0, H_{\text{ext}}=5$ T. (e) Contribution of D separated by a linear combination of (c) and (d). For details see text.

ment of the Mössbauer nucleus with $Q_{\text{Fe}} = +0.18$ b) at C sites were extracted (Table II). The central part of the spectra is poorly resolved, but does not show relaxation line broadening.

To separate the contributions from A and B in the low-

TABLE I. Quadrupole splittings (E_Q), isomer shifts (IS), linewidths (Γ), and relative intensities (A) of $\text{YBa}_2(\text{Cu}_{1-x}\text{M}_x)_3\text{O}_{7-y}$ (M : ^{57}Fe , ^{57}Co) at different temperatures with different x and y for doublets A, B, C, and D. E_Q , IS, and Γ in mm/s.

M	x	y	T (K)	A			B			C			D						
				E_Q	IS	Γ	A	E_Q	IS	Γ	A	E_Q	IS	Γ	A	E_Q	IS	Γ	A
^{57}Fe	0.1000	0.0	295	1.96	0.07	0.29	0.22 ^a	1.07	0.04	0.45	0.64	0.30	0.22	0.31	0.14 ^c				
	0.1000	0.0	85	2.01	0.16	0.29	0.22 ^a	1.09	0.13	0.48	0.64	0.29	0.30	0.33	0.14 ^c				
	0.1000	0.8	295	2.02	0.07	0.30	0.46 ^a	1.05	0.10	0.44	0.36	0.33	0.18	0.38	0.18 ^c				
	0.0600	0.0	295	1.96	0.05	0.29	0.33 ^a	1.10	0.02	0.41	0.55	0.33	0.22	0.27	0.12 ^c				
	0.0600	0.0	85	2.01	0.13	0.30	0.33 ^a	1.12	0.15	0.46	0.54	0.31	0.32	0.37	0.13 ^c				
	0.0600	0.8	295	2.03	0.08	0.31	0.58 ^a	1.07	0.12	0.43	0.26 ^b	0.32	0.17	0.35	0.16 ^c				
^{57}Co	0.0600	0.8	85	2.07	0.17	0.32	0.59 ^a	1.08	0.22	0.45	0.26 ^b	0.30	0.24	0.40	0.15 ^c				
	0.0100	0.0	295	1.98	0.03	0.26	0.21	1.09	-0.07	0.43	0.53	0.29	0.13	0.32	0.12	1.67	-0.04	0.37	0.14
	0.0100	0.0	85	2.00	0.14	0.26	0.24	1.09	0.09	0.44	0.53	0.22	0.30	0.22	0.12	1.73	0.01	0.42	0.11
	0.0015	0.0	295	2.00	0.02	0.22	0.10	1.10	-0.04	0.46	0.57	0.29	0.04	0.27	0.11	1.58	-0.14	0.24	0.22
	3.5×10^{-5}	0.0	295	2.05	0.02	0.41	0.33					0.58	0.21	0.35	0.10	1.44	-0.08	0.74	0.57
	3.5×10^{-5}	0.0	4.2	2.09	0.25	0.35	0.12					0.80	0.21	0.60	0.18	1.57	0.16	0.92	0.70
	3.5×10^{-5}	0.8	295	1.92	0.11	0.74	0.87					0.65	0.27	0.81	0.13				
	3.5×10^{-5}	0.8	4.2	1.97	0.13	0.92	0.92					0.80	0.15	0.60	0.08				

^aAsymmetry left/right: ≤ 1.15 .

^bAsymmetry left/right: ≥ 0.75 .

^cAsymmetry left/right: ≤ 1.40 .

^dVelocity scale reversed for better comparison.

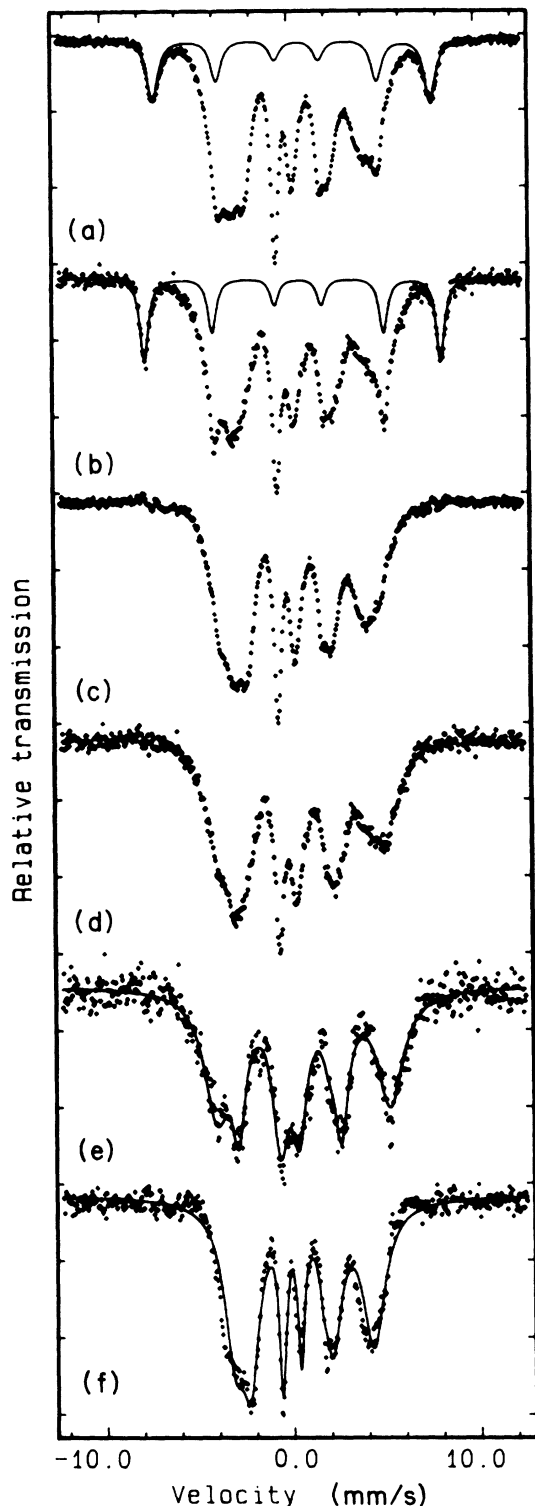


FIG. 3. Mössbauer absorption spectra of $\text{YBa}_2(\text{Cu}_{1-x}^{57}\text{Fe}_x)_3\text{O}_{7-y}$ at $T=4.2$ K. (a) $x=0.1$, $y \approx 0$, $H_{\text{ext}}=0$. (b) $x=0.1$, $y \approx 0.8$, $H_{\text{ext}}=0$. (c) and (d) spectra (a) and (b) after subtracting sextet of C. (e) Subspectrum A, and (f) subspectrum B. [(e) and (f) are the results of the linear combination of the spectra (c) and (d) with coefficients corresponding to the fractions of A and B in Figs. 1(b) and 1(a), respectively. For details see text.]

temperature Mössbauer spectra the following method was applied. First, contribution C was subtracted from both $y=0$ and $y=0.8$ spectra with an intensity ratio of 3:2:1 of the outer, middle, and inner lines of sextet C, respectively. Now it was assumed that the resulting normalized (by area) spectra in Figs. 3(c) and 3(d) were only composed of the components A and B with intensity fractions corresponding to the magnetically nonsplit spectra of Figs. 1(b) and 1(a). [Intensity fractions of A, B, and C do not show temperature dependence down to 85 K (see Table I); a trend that was extrapolated to 4.2 K.] Therefore, by making a channel by channel linear combination of the spectra in Figs. 3(c) and 3(d), the net contributions from A and B were determined [Figs. 3(e) and 3(f)]. Using values of the quadrupole splitting and isomer shift, extrapolated to 4.2 K, these spectra were further analyzed to extract $eQV_{zz}/2$, η (i.e., the asymmetry parameter of the EFG), H_{eff} , Φ , and θ , the azimuthal and polar angles of the effective magnetic field in the principal axes system of the EFG at the ^{57}Fe nucleus²⁴ located at A and B sites. Spectra of samples with $x_{\text{Fe}}=0.06$ were evaluated in the same manner. Solutions were found in a narrow region of values as shown in Table II. The sign of V_{zz} is positive and the asymmetry parameter is above 0.8 for both the A and B sites. Hasty conclusions are avoided at this point about the relative orientation of the crystal axes and the principal axes of EFG. With reference to unpublished data in a recent publication Blue *et al.*¹⁷ claim that V_{zz} is perpendicular to the crystallographic c axis and $\eta=0$ at site A. Our data, however, are indicative of $\eta>0.8$ for both $x_{\text{Fe}}=0.1$ and $x_{\text{Fe}}=0.06$ in case of both A and B. Further investigations on oriented crystallites in external magnetic fields are needed to resolve this discrepancy. It should be noted, however, that $\eta=0$ cannot be expected for Cu(1) sites, as their point symmetry is orthorhombic.

In order to determine the nature of the spontaneous magnetic order, external magnetic fields of 3 and 5 T were applied at various temperatures in a direction parallel to the incident gamma beam. If the order is ferromagnetic, a decrease of the overall splitting is expected. On the other hand, if it is antiferromagnetic, an increase of the linewidth and a small inside shift due to spin canting²⁵ is anticipated. Spectra without and with an external magnetic field of 5 T at 4.2 K are displayed in Figs. 4(a) and 4(b) showing a line broadening with a small inside shift of the outer lines. We, therefore, suggest this magnetic coupling to be of antiferromagnetic type.

Temperature variation of ^{57}Fe Mössbauer spectra of $\text{YBa}_2(\text{Cu}_{0.9}\text{Fe}_{0.1})_3\text{O}_7$ is displayed in Fig. 4. With increasing temperature, the decrease of the magnetic splitting for all subspectra is accompanied by relaxation line broadening, leading to a collapse of the magnetic splitting at lower temperatures than extrapolated from the temperature dependence of the overall splitting of subspectrum C. Relaxation spectra of $\text{YBa}_2(\text{Cu}_{1-x}\text{Fe}_x)_3\text{O}_{7-y}$ are treated in a separate publication.²⁶ The magnetic anisotropy energy of the clusters can be estimated from the onset temperature of spontaneous magnetic splitting, which is around 50 K for $x_{\text{Fe}}=0.1$. Due to the antiferromagnetic coupling, the net magnetic moment of the clusters is small (i.e., of the order of some Bohr magnetons). This net magnetic

TABLE II. Values of H_{eff} , $eQV_{zz}/2$, $\sin^2\theta$, $\cos(2\Phi)$, and η at 4.2 K for sites A , B , and C for $x_{\text{Fe}}=0.1$ and $x_{\text{Fe}}=0.06$. Values for $x_{\text{Fe}}=0.1$ correspond to the solid lines in Figs. 2(e) and 2(f) for subspectra A and B and in Figs. 2(a) and 2(b) for subspectrum C .

M	x	y	Doublet	H_{eff} (T)	$eQV_{zz}/2$ (mm/s)	$\sin^2\theta$	$\cos(2\Phi)$	η
^{57}Fe	0.10		A	≈ 27	+1.80	≈ 0.4	> 0.9	> 0.8
	0.06		A	≈ 26	+1.80	≈ 0.5	> 0.9	> 0.8
	0.10		B	≈ 23	+0.95	≈ 0.3	> 0.9	> 0.8
	0.06		B	≈ 21	+0.95	≈ 0.2	> 0.9	> 0.8
	0.10	0.0	C	46	-0.33 ··· -0.25	< 0.1		
	0.10	0.8	C	49	-0.33 ··· -0.25	< 0.1		
	0.06	0.0	C	44	-0.33 ··· -0.25	< 0.1		
	0.06	0.8	C	47	-0.33 ··· -0.25	< 0.1		

moment multiplied by an external magnetic field of 5 T is small compared to the anisotropy energy. Therefore, at temperatures of about 100 K, where the magnetic hyperfine splitting has collapsed, no magnetic stabilization of the antiferromagnetic subspectra is anticipated in an external magnetic field of 5 T. Since all subspectra show magnetic splitting of only 5 T, corresponding to the external magnetic field at 100 K [Figs. 4(e) and 4(f)], we conclude that all species are magnetically interrelated. This provides strong evidence of magnetic coupling between minority C and majority A and B sites. However, the onset temperature of spontaneous magnetic splitting of all species A , B , and C and also the extrapolated Néel temperatures for species C depend on y .²⁶

The above facts supply satisfactory evidence of superparamagnetic relaxation of small (antiferro-)magnetically ordered clusters²⁷ in $\text{YBa}_2(\text{Cu}_{1-x}\text{Fe}_x)_3\text{O}_{7-y}$ ($x_{\text{Fe}} > 0.01$). The existence of such small clusters of Fe or Co in $\text{YBa}_2(\text{Cu}_{1-x}\text{Fe}_x)_3\text{O}_{7-y}$ or $\text{YBa}_2(\text{Cu}_{1-x}\text{Co}_x)_3\text{O}_{7-y}$ is also in agreement with recent direct electron-diffraction results on Fe-doped samples.¹³

By examination of the values of isomer shift and magnetic hyperfine splitting, an attempt was made to determine the spin and valence state of the different species. Doublet C is unambiguously revealed by isomer shift, quadrupole splitting, and magnetic hyperfine splitting as high-spin Fe^{3+} . The most likely iron species corresponding to the subspectra A , B , and D is high-spin Fe^{4+} ($S=2$). Other species allowed by the isomer-shift data (diamagnetic iron, low-spin Fe^{2+} , low-spin Fe^{3+} , low-spin Fe^{4+}) can be ruled out on the basis of magnetic hyperfine splitting. On the other hand, intermediate spin Fe^{3+} ($S=\frac{3}{2}$) suggested by Takano and Takeda¹⁴ is unlikely on the basis of the isomer shift, which is typically 0.4 mm/s for Fe^{3+} ($S=\frac{3}{2}$).²⁸ The subspectra A and B have a magnetic hyperfine splitting of the same range. Therefore, if a spin state can be attributed to these partly covalent iron species at all, they have the same spin state. Temperature dependence of the central shift of A , B , and C is consistent with a second order Doppler shift having a slope of about -4.7×10^{-4} mm/s/K. This high value,²⁹ corresponding to an effective mass of 1.6 times the free-Fe ion mass, indicates relative loose bonding of the resonating nuclei to the lattice of $\text{YBa}_2\text{Cu}_3\text{O}_{7-y}$. The magnetic moment of Fe was found to be 4.78–4.88 μ_B in $\text{YBa}_2(\text{Cu}_{1-x}\text{Fe}_x)_3\text{O}_{7-y}$,³⁰ which is close to the spin-only value

for high-spin Fe^{4+} . These experimental data further support our assumption of high-spin Fe^{4+} .

Moreover, Demazeau *et al.* suggested a possible theoretical model for the stabilization of high-spin Fe^{4+} in similar perovskite structures³ via the elongation of the O_6 octahedra. Since the d -electron wave functions are of even parity, elongation of an oxygen octahedron along a C_4 axis (D_{4h} distortion) with a central $3d$ ion is identical with the removal of an axial oxygen from the octahedron followed by a possible shift of the metal atom inside the pyramid. Similarly, complete removal of axial oxygens can be modeled by introduction of a D_{4h} distortion in the octahedral crystal field. Even in a strong cubic crystal field, high-spin state of Fe^{4+} can be stabilized by a strong D_{4h} distortion.³¹

Comparing ^{57}Fe and ^{57}Co (low x) Mössbauer measurements, no aftereffect in emission spectra is found. Therefore, we suggest that Co is also mostly in the atypical Co^{4+} state in the 1:2:3 compound prior to the electron capture. If the electrons of the dopants simply fill the mixed-valence Cu band, the dependence of T_c on $3d$ substitution of Cu can be estimated. Now, we assume four-valent substitution of Cu in $\text{Y}^{3+}\text{Ba}_2^{2+}(\text{Cu}_{2+3x}^{2+}\text{Cu}_{1-6x}^{3+}\text{M}_{3x}^{4+})\text{O}_7$. The mixed-valence state of Cu linearly disappears at $x=\frac{1}{6}$. Assuming a mixed-valence state of oxygen we come to the same conclusion. This linear dependence in $\text{YBa}_2(\text{Cu}_{1-x}\text{M}_x)_3\text{O}_7$ ($M=\text{Fe}, \text{Co}$) is well supported by experimental zero-resistance midpoint temperatures of different authors reproduced in Fig. 5.

From the point of view of crystallographic assignment of species A to D we find it important that Mössbauer spectra of quenched samples and vacuum reduced ones are nearly identical.¹⁵ It is therefore unlikely that iron has a different atomic distribution (i.e., different site preference) in the oxidized (superconducting) and the reduced (nonsuperconducting) state due to diffusion during vacuum annealing.¹⁴ Moreover, we found that reducing and oxidizing is reversible from the point of view of T_c , Mössbauer parameters, and relative intensities. Simply on the basis of the above, and the diffraction evidence that Cu(1) sites are mostly affected on reduction of $\text{YBa}_2\text{Cu}_3\text{O}_{7-y}$, one should conclude that iron preferentially substitutes Cu(1). We believe that at least A and B sites, the most contributing to the Mössbauer spectra, may only differ in local symmetry, Fe–O bond length, or the number of oxygen neighbors, but both subspectra have to

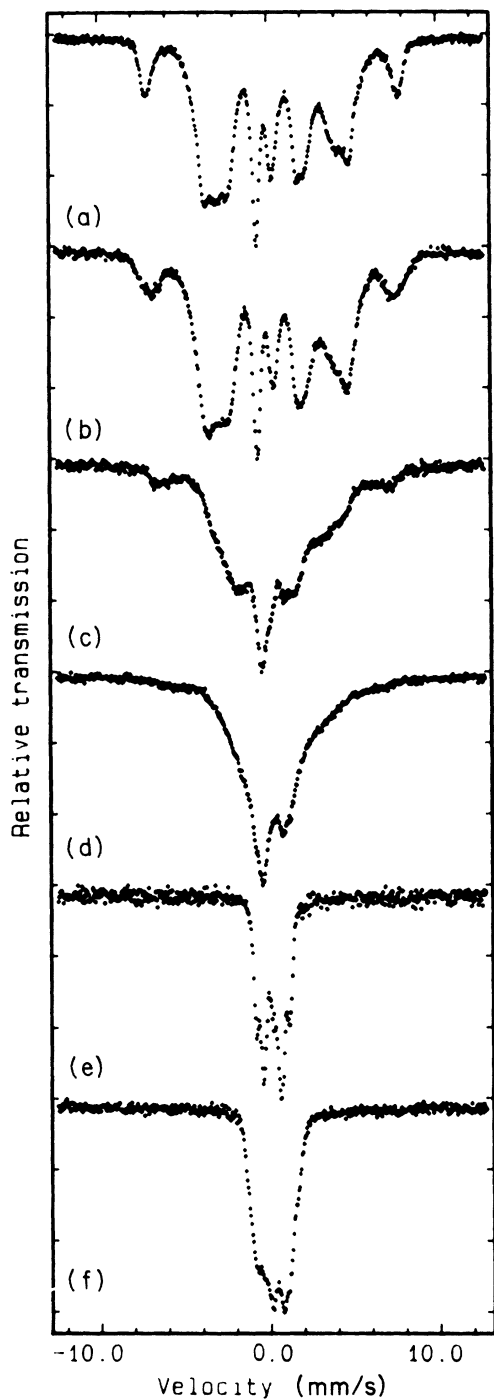


FIG. 4. Mössbauer absorption spectra of $\text{YBa}_2(\text{Cu}_{0.9}\text{Fe}_{0.1})_3\text{O}_7$ at different temperatures with and without applied magnetic field. (a) $T=4.2$ K, $H_{\text{ext}}=0$. (b) $T=4.2$ K, $H_{\text{ext}}=5$ T. (c) $T=15$ K, $H_{\text{ext}}=0$. (d) $T=19$ K, $H_{\text{ext}}=0$. (e) $T=100$ K, $H_{\text{ext}}=0$. (f) $T=100$ K, $H_{\text{ext}}=5$ T.

be assigned as Cu(1) sites. Furthermore, for $x_{\text{Fe}} \geq 0.06$ these Fe(1) sites are mostly neighboring sites allowing some kind of exchange interaction between iron atoms in small clusters.

Moreover, no spontaneous magnetic ordering is observed in $\text{YBa}_2(\text{Cu}_{1-x}\text{Co}_x)_3\text{O}_{7-y}$ with $x_{\text{Co}} = 3.5 \times 10^{-5}$

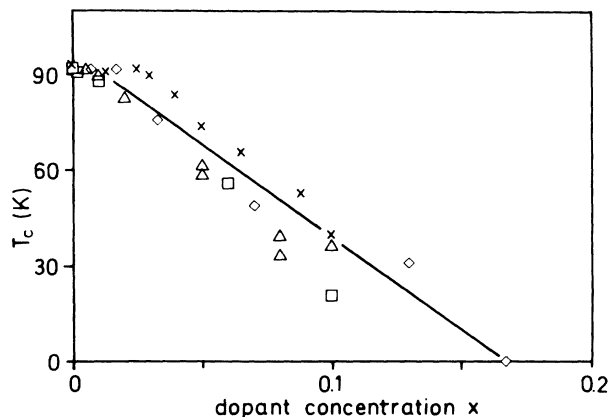


FIG. 5. Dependence of the zero-resistance midpoint temperature T_c on the dopant concentration in $\text{YBa}_2(\text{Cu}_{1-x}\text{M}_x)_3\text{O}_7$ ($M=\text{Fe}, \text{Co}$). T_c vs x_{Fe} (□), this work; (△), Ref. 32; (◇), Ref. 7; T_c vs x_{Co} (×), Ref. 11. Solid line assumes a linear depression of T_c on increasing four-valent dopant concentration in $\text{Y}^{3+}\text{Ba}_2^{2+}(\text{Cu}_{2+3x}^{2+}\text{Cu}_{1-6x}^{3+}\text{M}_{3x}^{4+})\text{O}_7$ (see text).

at 4.2 K, but the species *A* and *D* show paramagnetic behavior in an applied magnetic field of 5 T. Thus, it seems reasonable to assign *D* to isolated Fe sites, which can transform to (isolated) *A* sites on reduction. *A* sites are characteristic of the $\text{YBa}_2\text{Cu}_3\text{O}_{7-y}$ matrix rather than of the clusters themselves.

The reason for such clustering is not understood at present. It is tempting to argue that the square planar Cu(1) coordination is very atypical of iron. According to Bordet *et al.*,¹³ iron preferentially occupies the possibly distorted tetrahedral, pyramidal, and octahedral sites formed by two O(4), one O(1), and one occupied O(5), two O(4), two O(1), and one occupied O(5) or two O(4), two O(1), and two occupied O(5), respectively, along the twin boundaries in the [110] and $[-110]$ directions in $\text{YBa}_2(\text{Cu}_{1-x}\text{M}_x)_3\text{O}_{7-y}$. However, $\text{YBa}_2(\text{Cu}_{1-x}\text{Fe}_x)_3\text{O}_{7-y}$ of x - and y -induced tetragonality may have markedly different oxygen stoichiometry in the Cu(1) plane. Since superparamagnetic cluster formation is established also in our reduced samples for $x_{\text{Fe}} \geq 0.06$, where, due to y -type tetragonality, twinning need not exist, such a driving force for [110] ordering is questionable.

The increase of the overall oxygen stoichiometry on doping of $\text{YBa}_2(\text{Cu}_{1-x}\text{Fe}_x)_3\text{O}_{7-y}$ by Fe or Co is well established.^{8,12,13} The certainly superexchange-mediated antiferromagnetic order persisting at Fe(1) sites in the reduced state may be independent evidence of the existence of excess oxygen in $\text{YBa}_2(\text{Cu}_{1-x}\text{Fe}_x)_3\text{O}_{7-y}$, which is, however, a contradiction to the assignment of Blue *et al.*¹⁷

From our results we suggest that *B* and *D* are pyramidal sites in Cu(1) position. Sensitivity of these shifted species to next-nearest-neighbor effects in the EFG may account for the observed line broadening of the corresponding quadrupole doublets. On reduction, *B* and *D* sites transform to fourfold coordinated (possibly square planar) sites, which we assign to doublet *A*. The difference in charge transfer between neighboring Fe and between Fe and Cu may account for the more negative

isomer shift of the isolated *D* species. The unexpectedly small difference in the isomer shifts of *A* and *B* may be due to charge transfer between Cu(1) and Cu(2) layers in the higher *x* case.⁸ Values of the asymmetry parameter of the EFG imply a strong distortion at *A* and *B* sites, which may also be due to this charge transfer. However, it is difficult to explain why Fe and Co prefer a square planar Cu(1) coordination to Cu(2) which is also a pyramidal (practically square planar) fourfold coordinated site. One solution might be that iron or cobalt, substituting lower valent Cu(2)²⁺, insist on having a sixth oxygen to complete the octahedron. The excess oxygen brought in the vicinity of the rare earth may be energetically unfavorable, which in turn explains Fe(1) preference over Fe(2), the latter of which we therefore identify as the low-intensity *C* species. Magnetic coupling of species *C* to clusters in Cu(1) positions implies exchange interactions via O(4). Further investigations will clarify this point.

CONCLUSIONS

In conclusion, four Fe species are needed for a consistent interpretation of *x* and *y* dependence of Mössbauer spectra of YBa₂(Cu_{1-x}Fe_x)₃O_{7-y} in the oxidized and reduced state.

Spontaneous antiferromagnetic order is observed at 4.2 K in samples with *x*_{Fe}=0.06 and *x*_{Fe}=0.1, unlike in the low-concentration ones with *x*_{Fe}=0.01 and *x*_{Co}=3.5 × 10⁻⁵, which are paramagnetic at 4.2 K. For *x*_{Fe}=0.1 and *x*_{Fe}=0.06, all subspectra are practically static at 4.2 K. Net contribution of *A* and *B* was determined by a linear combination method. *η*, the asymmetry parameter

of the EFG, is above 0.8 and *V*_{zz} is positive for both *A* and *B* species. For *C*, *V*_{zz} is negative, while for *D* it is probably positive.

Temperature variation and magnetic field dependence of magnetically split spectra are indicative of superparamagnetic relaxation of antiferromagnetically ordered small clusters at *x*_{Fe}=0.1 and *x*_{Fe}=0.06. This relaxation has a common characteristic temperature for the subspectra *A*, *B*, and *C*. Therefore, we suggest the *A*, *B*, and *C* sites to be magnetically interrelated.

From our results we conclude that the species *A*, *B*, and *D* are high-spin Fe⁴⁺, *C* is high-spin Fe³⁺. We provide evidence that Co is also mostly in a four-valent state. In case of Fe, a strong *D*_{4h} distortion of the *M*(1) environment is a possible explanation of this rather rare valence state. Four-valent Fe and Co substitution in YBa₂Cu₃O_{7-y} is in reasonable agreement with the dopant concentration dependence of *T*_c.

We suggest that majority species *B* and *D* are pyramidally coordinated Cu(1) sites, *C* is a Cu(2) site, and *A* is a fourfold coordinated, probably square planar Cu(1) site.

ACKNOWLEDGMENT

Fruitful discussions with Dr. H. Adrian, Dr. Gy. Huttiray, Dr. O. Leupold, Dr. L. Mihály, and conductivity measurements by G. Oszlányi are gratefully acknowledged. This work was partly supported by the Deutsche Forschungsgemeinschaft, by the Hungarian Academy of Sciences, and by OMFB, the Hungarian National Committee of Technical Development.

¹T. Siegrist, S. Sunshine, D. W. Murphy, R. J. Cava, and S. M. Zahurak, *Phys. Rev. B* **35**, 7137 (1987).

²S. Sato, I. Nakada, T. Kohara, and Y. Oda, *Jpn. J. Appl. Phys.* **26**, L663 (1987).

³J. D. Jorgensen, M. A. Beno, D. G. Hinks, L. Soderholm, K. J. Volin, R. L. Hitterman, J. D. Grace, I. K. Schuller, C. U. Segre, K. Zhang, and M. S. Kleefisch, *Phys. Rev. B* **36**, 3608 (1987).

⁴H. A. Borges, R. Kwok, J. D. Thompson, G. L. Wells, J. L. Smith, Z. Fisk, and D. E. Peterson, *Phys. Rev. B* **36**, 2404 (1987).

⁵T. P. Orlando, K. A. Delin, S. Foner, E. J. McNiff, Jr., J. M. Tarascon, L. H. Greene, W. R. McKinnon, and G. W. Hull, *Phys. Rev. B* **36**, 2394 (1987).

⁶T. R. Dinger, T. K. Worthington, W. J. Gallagher, and R. L. Sandstrom, *Phys. Rev. Lett.* **58**, 2687 (1987).

⁷J. M. Tarascon, P. Barboux, P. F. Miceli, L. H. Greene, G. W. Hull, M. Eibschutz, and S. A. Sunshine, *Phys. Rev. B* **37**, 7458 (1988).

⁸P. F. Miceli, J. M. Tarascon, L. H. Greene, P. Barboux, F. J. Rotella, and J. D. Jorgensen, *Phys. Rev. B* **37**, 5932 (1988).

⁹J. Jung, J. P. Franck, W. A. Miner, and M. A.-K. Mohamed, *Phys. Rev. B* **37**, 7510 (1988).

¹⁰Y. Maeno, M. Kato, Y. Aoki, and T. Fujita, *Jpn. J. Appl. Phys.* **26**, L1982 (1987).

¹¹J. Langen, M. Veit, M. Galfy, H.-D. Jostarndt, A. Erle, S.

Blumenröder, H. Schmidt, and E. Zirngiebl, *Solid State Commun.* **65**, 973 (1988).

¹²G. Roth, G. Heger, B. Renker, J. Pannetier, V. Caignaert, M. Hervieu, and B. Raveau, *Z. Phys. B* **71**, 43 (1988).

¹³P. Bordet, J. L. Hodeau, P. Strobel, M. Marezio, and A. Santoro, *Solid State Commun.* **66**, 435 (1988).

¹⁴M. Takano and Y. Takeda, *Jpn. J. Appl. Phys.* **26**, L1862 (1987).

¹⁵E. Baggio-Saitovitch, I. Souza Azevedo, R. B. Scorzelli, H. Saitovitch, S. F. da Cunha, A. P. Guimaraes, and A. Y. Takeuchi, *Phys. Rev. B* **37**, 7971 (1988).

¹⁶Some results of emission Mössbauer spectroscopy were already presented at the Melbourne Mössbauer Conference (1987).

¹⁷C. Blue, K. Elgaid, I. Zitkovsky, P. Boolchand, D. McDaniel, W. C. H. Joiner, J. Oostens, and W. Huff, *Phys. Rev. B* **37**, 5905 (1988).

¹⁸E. R. Bauminger, M. Kowitt, I. Felner, and I. Nowik, *Solid State Commun.* **65**, 123 (1988).

¹⁹Z. Q. Qiu, Y. W. Du, H. Tang, J. C. Walker, W. A. Bryden, and K. Moorjani, *J. Magn. Magn. Mater.* **69**, L221 (1987).

²⁰Q. A. Pankhurst, A. H. Morrish, and X. Z. Zhou, *Phys. Lett. A* **127**, 231 (1988).

²¹T. Tamaki, T. Komai, A. Ito, Y. Maeno, and T. Fujita, *Solid State Commun.* **65**, 43 (1988).

²²J. J. Bara, B. F. Bogacz, A. Szytula, and Z. Tomkowicz, *Solid*

- State Commun. **66**, 431 (1988).
- ²³P. A. Flinn, S. L. Ruby, and W. L. Kehl, *Science* **143**, 1434 (1964).
- ²⁴H. Spiering, *Habilitationsschrift*, Universität Erlangen-Nürnberg, 1978 (unpublished), p. 7.
- ²⁵V. Beckmann, W. Bruckner, W. Fuchs, G. Ritter, and H. Wegener, *Phys. Status Solidi* **29**, 781 (1968).
- ²⁶J. Dengler, G. Ritter, J. Schober, L. Bottyán, B. Molnár, D. L. Nagy, and I. S. Szücs (unpublished).
- ²⁷S. Mørup, *Paramagnetic and Superparamagnetic Relaxation Phenomena Studied by Mössbauer Spectroscopy* (Polyteknisk Forlag, Lyngby, Denmark, 1981).
- ²⁸E. König, G. Ritter, J. Waigel, L. F. Larkworthy, and R. M. Thompson, *Inorg. Chem.* **26**, 1563 (1987).
- ²⁹E. König, G. Ritter, S. K. Kulshreshtha, and S. M. Nelson, *J. Am. Chem. Soc.* **105**, 1924 (1983).
- ³⁰J. Jing, J. Bieg, H. Engelmann, Y. Hsia, U. Gonser, P. Gütlich, and R. Jakobi, *Solid State Commun.* **66**, 727 (1988).
- ³¹G. Demazeau, M. Pouchard, N. Chevreau, M. Thomas, F. Ménil, and P. Hagenmuller, *Mater. Res. Bull.* **16**, 689 (1981).
- ³²Y. Oda, H. Fujita, H. Toyoda, T. Kaneko, T. Kohara, I. Nakada, and K. Asayama, *Jpn. J. Appl. Phys.* **26**, L1660 (1987).